Closed Loop Input Current Control of a Hybrid 12-Pulse Rectifier

J. Biela, D. Hassler, J. Schönberger and J. W. Kolar

ETH Zurich, Power Electronic Systems Laboratory
Physikstrasse 3, CH-8092 Zurich, Switzerland

***Abstract*—This paper presents a novel closed loop current control strategy for a hybrid 12-pulse rectifier that uses a two-switch boost stage for output voltage regulation. Unlike previous attempts to mitigate input current distortion, e.g. by injecting voltages on the rectifier output side in open loop control mode, this new closed loop current control scheme directly controls the input current space vector and/or impresses sinusoidal input currents. In this paper, the control strategy is explained and the modulation functions for each $\frac{\pi}{3}$-wide mains voltage sector are derived. The hardware implementation is described, and experimental results demonstrate that the control strategy ensures a high quality input current for ideal or distorted/unbalanced mains.**

***Index Terms*—12-pulse rectifier, current control, space vector modulation**

I. Introduction

In aerospace applications, where drive systems are connected to the on-board electrical system, rectifiers with a high input current quality are required in order to limit the distortions. There, basically line commutated systems with a high pulse number [1], [2] or active systems, i.e. PWM-rectifiers with controlled input current, can be applied. Due to the high mains frequency of 360Hz to 800Hz, the low cooling effort, and the missing EMI-filter passive 12-pulse rectifiers without galvanic isolation achieve similar power densities than active rectifiers systems [3]. Furthermore, passive systems have a high pulse load capability and a low complexity. However, the passive 12-pulse rectifier is not without drawbacks. E.g. no output voltage regulation is provided, and/or the drive system has to be designed for the lowest possible mains voltage, what leads to an oversized motor. Furthermore, the input current contains low order harmonics.

One attempt to address the issue of voltage regulation is based on a hybrid 12-pulse rectifier with an LIT and a two-switch interleaved boost output stage [4] as shown in Fig. 1. In the simplest case an approximately constant duty cycle is used for output voltage regulation, while

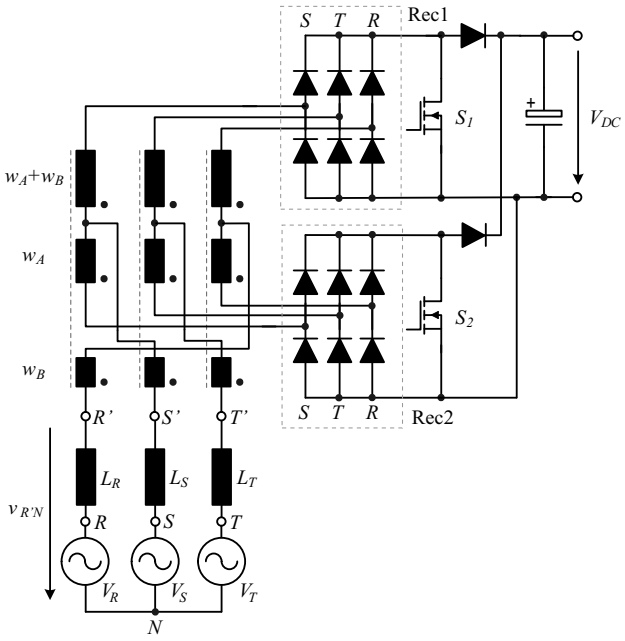

Fig. 1: Two-switch hybrid 12-pulse rectifier with Line Interface Transformer (LIT).

the required current carrying capability of the switches is low. In order to achieve sinusoidal input currents besides output voltage control, a modulation of the duty cycles is necessary. There, an output voltage of approximately twice the value given for purely passive operation is required, which is no drawback for drive systems in the higher power region. Consequently, a sinusoidal input current could be achieved without employing a complex 18- or 24-pulse line interface transformer (LIT). Furthermore, the value of the mains side inductors L_ν,

TABLE I: Specification of the 10kW prototype system

Input Voltage range	115V± 15% ≈ 98 - 132V_{RMS}
Input frequency range	360-800Hz
Input Inductor	188μH
LIT	$w_A + w_B : w_A : w_B$= 29:21:8
Output Power	10kW
Nominal V_{Out}	250V (passive) / 520V (closed loop)

$\nu = R, S, T$, could be reduced due to high switching frequency.

However, for a purely open loop controlled modulation of the two switches a distortion or unbalance of the mains voltage would result in distorted or unbalanced input currents. Therefore, a closed loop input current control, which ensures sinusoidal input currents also for distorted/unbalanced mains voltages, is presented in this paper. In section II the operating principle of the control concept which is based on space vector modulation is explained and the derivation of the modulation functions is shown. The implementation of the controller is described in detail in section III. Experimental results given in section IV verify the theoretical considerations and demonstrate the good performance of the proposed concept.

II. Space Vector Modulation

For purely passive operation of, i.e. switches S_1 and S_2 remaining in the turn-off state, the system depicted in Fig.1 shows a 12-pulse input current shape with a THD of 6.5%. This 12-pulse operation results due to the 30° phase shifted operation of the two rectifier stages, which is caused by the Line Interface Transformer (LIT) [5]. The LIT is assumed to have an ideal coupling of the related windings in a first approximation in the following (further details see section II-A).

In order to reduce the low frequency harmonics and/or the THD of the input current, i.e. for providing sinusoidal input currents the two switches must be controlled in a way, that the local average of the voltage across the boost inductors $L_{b,\nu}$ exhibits a sinusoidal shape. Since the mains' star point N is not connected to the rectifier system/load, the sum of the three mains currents is forced to zero $\sum i_{N,i} = 0$ and the zero sequence component of the boost inductor voltage

$$v_{L,0} = \frac{1}{3}\left(v_{L,R} + v_{L,S} + v_{L,T}\right) \tag{1}$$

does not influence the phase currents. Consequently, the current in the boost inductors is defined by

$$\underline{v}_L = L\frac{\underline{i}_N}{dt} = \underline{v}_N - \underline{v}_{LIT}, \tag{2}$$

where $\underline{v}_N$ is the space vector of the mains voltage

$$\underline{v}_N = \widehat{V}_N e^{j\varphi_N} \text{ with } \varphi_N = \omega_N t \tag{3}$$

and

$$\underline{v}_{LIT} = \frac{2}{3}\left(v_{R'N} + \underline{a}v_{S'N} + \underline{a}^2 v_{T'N}\right) \quad \text{with } \underline{a} = e^{j\frac{2\pi}{3}} \tag{4}$$

is the space vector at the input of the LIT (R', S' and T').

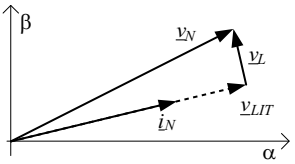

Fig. 2: Calculation of input current reference space vector $\underline{i}_N$.

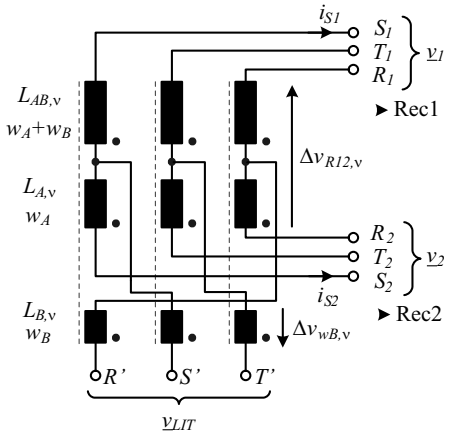

Fig. 3: Calculation of the voltage transfer function of an ideal LIT.

For calculating the reference space vector $\underline{v}^*_{LIT}$ resulting in sinusoidal input currents, the phase of the input current space vector $\underline{i}^*_N$ is required. Due to the ohmic behaviour of the three phase rectifiers $Rec1$ and $Rec2$ [3], which is transferred via the ideal LIT to nodes R', S' and T', the reference vector $\underline{i}^*_N$ for the input current must be aligned with $\underline{v}_{LIT}$ (cf. Fig. 2). Thus, $\underline{i}^*_N$ could be defined as

$$\underline{i}^*_N = \widehat{I}^*_N e^{j\varphi_I} \quad \text{with } \varphi_I = arctan\left(\frac{\widehat{v}_L}{\sqrt{\widehat{V}_N^2 - \widehat{v}_L^2}}\right) \tag{5}$$

resulting in a reference vector $\underline{v}^*_{LIT}$,

$$\underline{v}^*_{LIT} = \widehat{V}^*_{LIT} e^{j\varphi_I} \quad \text{with } \widehat{V}_{LIT} = \sqrt{\widehat{V}_N^2 - \widehat{v}_L^2}, \tag{6}$$

which is generated in the time average over a switching period T_P.

In order to calculate the relative on times $\delta_{\mu\nu}$ of S_1 and S_2, first the space vectors $\underline{v}_{LIT}$, which can be generated by switching S_1 and S_2, are calculated based on Fig. 3. There, the mesh equation

$$\underline{v}_{LIT} = \underline{v}_2 - \Delta\underline{v}_{wB} + \frac{w_A}{2w_A + w_B}\Delta\underline{v}_{R12} \tag{7}$$

could be set up, where $\Delta\underline{v}_{R12}$ is the space vector of the voltage $\Delta v_{R12,\nu}$ between the two rectifiers. By assuming an ideal coupling of the LIT the voltages $\Delta v_{wB,\nu}$ across

the inductors $L_{B,\nu}$ can be expressed by

$$\begin{aligned}\Delta v_{wB,R} &= \frac{w_B}{2w_A + w_B}\Delta v_{R12,S}\\ \Delta v_{wB,S} &= \frac{w_B}{2w_A + w_B}\Delta v_{R12,T}\\ \Delta v_{wB,T} &= \frac{w_B}{2w_A + w_B}\Delta v_{R12,R},\end{aligned} \tag{8}$$

which reveals that the voltages are phase shifted, due to the rotated connection of $L_{B,\nu}$ to $L_{A,\mu}$ and $L_{AB,\mu}$. With (8) the space vector $\Delta\underline{v}_{wB}$ could be simplified to

$$\begin{aligned}\Delta\underline{v}_{wB} &= \frac{2}{3}\left(\Delta v_{wB,R} + \underline{a}\Delta v_{wB,S} + \underline{a}^2\Delta v_{wB,T}\right) \qquad (9)\\ &= \frac{2}{3}\frac{w_B}{2w_A+w_B}\left(\Delta v_{R12,S}+\underline{a}\Delta v_{R12,T}+\underline{a}^2\Delta v_{R12,R}\right).\end{aligned}$$

By multiplying this result by $\frac{\underline{a}}{\underline{a}}$ (10) results in

$$\begin{aligned}\Delta\underline{v}_{wB} &= \frac{w_B}{2w_A + w_B}\Delta\underline{v}_{R12}\frac{1}{\underline{a}}\\ &= \frac{w_B}{2w_A + w_B}\Delta\underline{v}_{R12}e^{j\frac{-2\pi}{3}}.\end{aligned} \tag{10}$$

Consequently, the space vector $\Delta\underline{v}_{wB}$ is formed by scaling and rotation of $\Delta\underline{v}_{R12}$ by 120°. With this result the mesh equation (7) could be simplified to

$$\begin{aligned}\underline{v}_{LIT} &= \underline{v}_2 - \frac{w_B}{2w_A + w_B}\underline{a}^2\Delta\underline{v}_{R12} + \frac{w_A}{2w_A + w_B}\Delta\underline{v}_{R12}\\ &= \underline{v}_2 + (\underline{v}_1 - \underline{v}_2)\left(\frac{w_A - w_B\underline{a}^2}{2w_A + w_B}\right),\end{aligned} \tag{11}$$

which allows the calculation of $\underline{v}_{LIT}$ in dependence of the input voltage space vectors $\underline{v}_1$ and $\underline{v}_2$ of the rectifiers. $\underline{v}_1$ and $\underline{v}_2$ are defined by the switching state and the sign of the rectifier input currents $i_{\nu 1}$ and $i_{\nu 2}$ (cf. Fig. 4). Due to the 30° $\left(\frac{\pi}{6}\right)$ phase shift of the two rectifier phase current systems, there are 12 different combinations of current signs, which are defining 12 sectors as shown in Fig. 4.

In each sector four possible switching states are given: (00), (01), (10) and (11). In case of (11) both switches are turned on resulting in $\underline{v}_1 = \underline{v}_2 = 0$, and $\underline{v}_{LIT} = 0$ and/or in an increasing inductor current. This state could be used for boosting the output voltage.

In state (00) both switches are off and the rectifier behaves like a purely passive 12-pulse rectifier. In the two active states (01) ($\rightarrow$ S_1=off, S_2=on) and (10), where only one switch is turned on, the two space vectors $\underline{v}_{LIT(01)}$ and $\underline{v}_{LIT(10)}$, which are rotated by $\pm 15°$ ($\pm\pi/12$) with respect to vector $\underline{v}_{LIT(00)}$, can be formed (cf. Fig. 5). By means of vectors $\underline{v}_{LIT(00)}$, $\underline{v}_{LIT(01)}$ and $\underline{v}_{LIT(10)}$ any reference vector in the triangle defined by the voltage vectors could be generated in time average over a pulse period. Accordingly, also purely sinusoidal

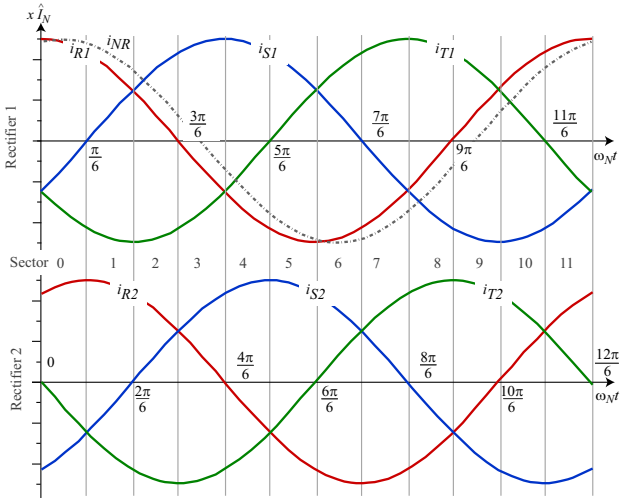

Fig. 4: Sector definition in dependence of ideal rectifier currents.

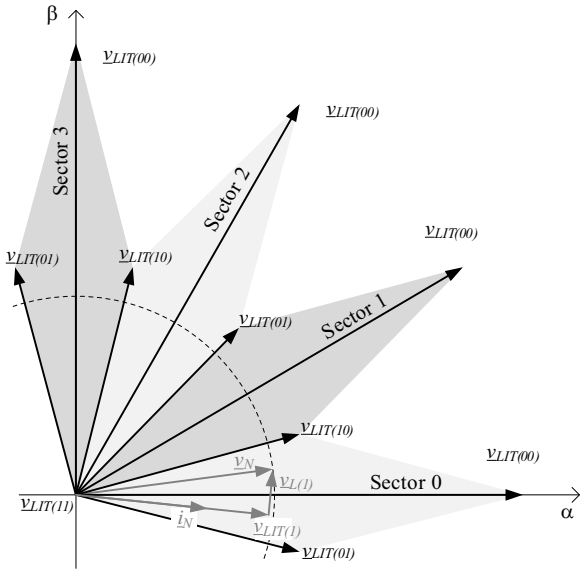

Fig. 5: Space vectors which can be generated by the rectifier system.

voltages $v_{\nu' N}$, which result in sinusoidal input currents, can be generated by the space vector modulation.

The reference voltage vector is formed by geometrically adding the rectifier voltage space vectors

$$\underline{v}^*_{LIT} = \underline{v}_{LIT(1)} = \delta_{(10)}\underline{v}_{LIT(10)} + \delta_{(11)}\underline{v}_{LIT(11)} + \delta_{(01)}\underline{v}_{LIT(01)} \tag{12}$$

weighted by the relative on-times δ_j of the switching states $j = (s_1, s_2)$. These on-times can be calculated from simple geometrical considerations and are a function of the angle θ_{LIT} of $\underline{v}^*_{LIT}$ and of the magnitude

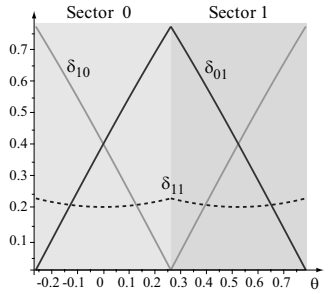

Fig. 6: Time behaviour of the relative on-times δ_{11}, δ_{01} and δ_{10} for sectors 0 and sector 1.

$|\underline{v}^*_{LIT}| = \widehat{V}^*_{LIT}$. The resulting on-times for sector 0 are

$$\delta_{(11)} = 1 - 3\frac{\widehat{V}^*_{LIT}}{V_{DC}}\cos\theta_{LIT} \tag{13}$$

$$\delta_{(01)} = \frac{3}{2}\frac{\widehat{V}^*_{LIT}}{V_{DC}}\left(\cos\theta_{LIT} + \left(2+\sqrt{3}\right)\sin\theta_{LIT}\right) \tag{14}$$

$$\delta_{(10)} = \frac{3}{2}\frac{\widehat{V}^*_{LIT}}{V_{DC}}\left(\cos\theta_{LIT} - \left(2+\sqrt{3}\right)\sin\theta_{LIT}\right). \tag{15}$$

Similar equations can be derived for the other sectors. In spite of that, it is also possible to rotate the reference vector $\underline{v}^*_{LIT}$ always back to sector 0. There, the relative angles of $\underline{v}^*_{LIT}$ to the sector borders must be retained. Furthermore, it is important to note that in odd-numbered sectors, the switching vectors $\underline{v}_{LIT(01)}$ and $\underline{v}_{LIT(10)}$ are transposed, so that the relative on-times also must be transposed.

For a simpler implementation of the equations for the relative on-times in a DSP, an approximation

$$\delta_{(01)} = \frac{\widehat{V}^*_{LIT}}{V_{DC}}\left(\frac{3}{2} + \frac{18}{\pi}\theta\right) \tag{16}$$

$$\delta_{(10)} = \frac{\widehat{V}^*_{LIT}}{V_{DC}}\left(\frac{3}{2} - \frac{18}{\pi}\theta\right) \tag{17}$$

$$\delta_{(11)} = 1 - \delta_{(01)} - \delta_{(10)} \tag{18}$$

could be utilised. In Fig. 5 the time behaviour of the relative on-times is shown for sectors 0 and 1. With (13), (14) and (15) it is now possible to generate arbitrary space vectors at the input of the LIT, which are located inside the triangle $\underline{v}_{LIT(00)}$, $\underline{v}_{LIT(01)}$ and $\underline{v}_{LIT(10)}$. The reference for the space vector is determined by the current controller, which is described in the following section.

A. Line Interface Transformer

So far, an ideal coupling of the LIT has been assumed for the derivation of the equations. In practice, however, due to the leakage flux the coupling coefficient is always lower than one. Assuming three identical LITs for the three phases, i.e. the coupling coefficients are the same for all three LITs, the resulting leakage inductances can be transferred to R', S' and T' (cf. Fig. 3), so that they act as if they would be connected in series to the boost inductors. The value of the therefore resulting additional boost inductance $L_{b,add}$ is

$$\begin{aligned} L_{b,add} = \Big[& L_A\sqrt{L_B L_{AB}}\,(K_{AB,A}K_{A,B} - K_{AB,B}) - \\ & 2L_B\sqrt{L_A}\,(K_{A,B}K_{AB,B} - K_{AB,A}) + \\ & L_{AB}\sqrt{L_B L_A}\,(K_{A,B} - K_{AB,A}K_{AB,B}) + \\ & L_{AB}\left(L_A - K^2_{AB,B}L_B - K^2_{AB,A}L_A + L_B\right) + \\ & L_A L_B\left(1 - K^2_{A,B}\right)\Big] / \\ & \left[L_A + 2K_{AB,A}\sqrt{L_A L_{AB}} + L_{AB}\right], \end{aligned} \tag{19}$$

where $K_{\nu,\lambda}$ is the coupling coefficient between two respective inductors.

In case the coupling coefficients between the three inductors are not equal the currents in the two rectifiers become slightly unbalanced, but the additional inductances seen at the port R', S' and T' are still equal for all three phases. In case the three LITs are not identical, i.e. the coupling coefficients/inductance of the three LITs are different, the currents of the two rectifiers are unbalanced and the additional inductances in the three phases are not identical any more. Slight asymmetric values of the indutors/coupling coefficients can be compensated by the controller presented in the following section without impairing the line current, but larger deviations will lead to a distorted mains current.

III. Controller

Based on the space vector modulation described in the previous section, the control structure shown in Fig. 7 has been derived. There, a Phase-Locked-Loop (PLL) controller is used to determine the d-component and the phase angle θ_N of the line voltage V_N, while the q-component of V_N is regulated to zero. With θ_N also the d- and the q- component of the line current are calculated. These values are compared with their reference values $I^*_N\cos\theta_{ref,P}$ and $I^*_N\sin\theta_{ref,P}$ and the difference is fed into the PI-controllers for the d- and the q-component of the line current.

The reference value I^*_N is determined by a voltage controller (not shown in Fig. 7 for simplicity), which regulates the output voltage, or fixed by the user and the angle $\theta_{ref,F}$ between the mains voltage vector $\underline{v}_N$ and the reference current vector $\underline{i}_N$ is calculated using

$$\theta_{ref,F} = \arctan\frac{\omega L I^*_N}{\sqrt{v^2_{N,d} - \omega L I^*_N}}, \tag{20}$$

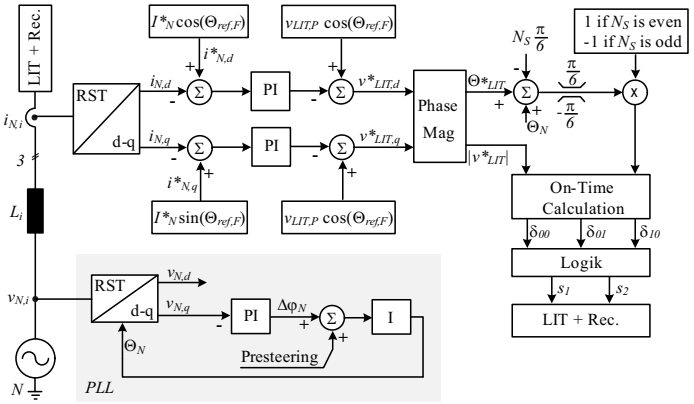

Fig. 7: Basic structure of the controller for the 12-pulse rectifier system with sinusoidal input currents and output voltage regulation.

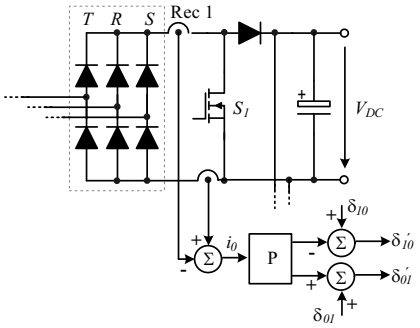

Fig. 8: Controller for limiting the circulating zero sequence current in $L_{A,\nu}$, $L_{AB,\nu}$, $Rec1$ and $Rec2$.

which could be derived from Fig. 2. The feed-forward signals $v_{LIT,F}\cos\theta_{ref,F}$ and $v_{LIT,F}\sin\theta_{ref,F}$ for the d- and the q- component are added to the controller output. The amplitude $v_{LIT,F}$ is given by

$$v_{LIT,F} = \sqrt{v_{N,d}^2 - \omega L I_N^*}, \tag{21}$$

and can be derived by means of Fig. 3. After the summation the d- and the q- component of the reference vector $v_{LIT,d}^*$ and $v_{LIT,q}^*$ are given and the amplitude $|v_{LIT}^*|$ and the angle θ_{LIT}^* of the reference vector for the input voltage of the LIT are calculated.

In the next step the reference vector is rotated back to sector 0 by adding the mains phase angle θ_N and subtracting $N_s\frac{\pi}{6}$ to θ_{LIT}^*. N_s is the number of the current sector in which the reference current lies. Usually, the result should be within the allowed region $\pm15°$ $(\pm\frac{\pi}{6})$, which is determined by the sector borders. In order to eliminate numerical/measurement errors the angle is limited to $\pm15°$. Thereafter, the angle is multiplied by 1 if the sector N_s is even and by -1 if N_s is odd in order to obtain a triangular reference angle which starts at $-15°$ rises up to $15°$ and then ramps down to $-15°$ again instead of a sawtooth-like angle, which jumps to $-15°$ as soon as it reaches $15°$. This time behaviour of the reference angle is required to obtain modulation signals as shown in Fig. 6, which can be calculated using (13), (14) and (15).

In the 12-pulse rectifier system shown in Fig. 1 a circulating zero sequence current is flowing via L_A, L_{AB}, $Rec1$, the output capacitor and $Rec2$ [5], which is driven by the voltage difference between $Rec1$ and $Rec2$ due to the $30°$ phase shift. Due to the phase shift this current is intrinsic for this kind of 12-pulse system and could not be reduced without impairing the mains current quality. However, the amplitude of the current could increase in case of unequal switching times and offsets. Therefore, an additional control loop is implemented for limiting the zero sequence current.

There, the zero sequence current is measured by subtracting the currents in the positive and negative rail of $Rec1$. The result is amplified and then added to/subtracted from the relative on-times of states (01) and (10), implementing a P-type control. In order not to impair the THD of the mains current the gain of the P-controller has to be limited to low values.

IV. Measurement Results

In order to validate the presented closed loop control strategy, a 10kW prototype system with a switching frequency of 60kHz was constructed. The main components are listed in Table II. A photo of the experimental system is shown in Fig. 9.

The prototype system comprises two PCBs with the input inductors and LIT mounted beneath on the chassis. The main power PCB not only hosts the power circuit, but also an auxiliary power supply, a pre-charge circuit, and analog measurement and level-shifting circuits for use by the DSP control board. The control board, based on a Texas Instruments TMS320F2808 fixed-point DSP

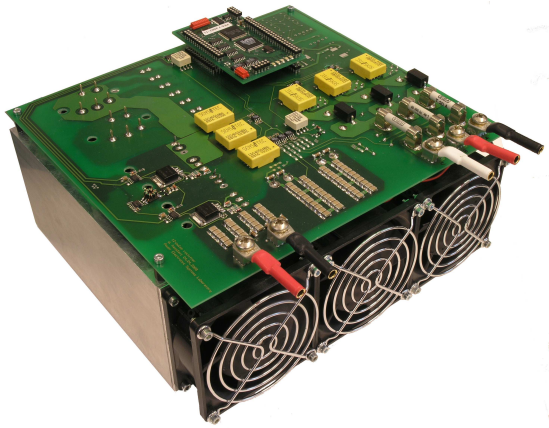

Fig. 9: Photo of the hardware prototype (24cm×22×10cm).

TABLE II: Components for 10kW prototype system

Component	Parameter
Input inductor	188μH Core: S3U 48b / Trafoperm N2/0.1mm
LIT	$w_A + w_B : w_A : w_B$= 29:21:8 Core: 2×SM65 / Trafoperm N2/0.1mm L_{AB}=5.2mH, L_A=2.5mH, L_B=0.35mH
Current sensors	Sensitec CMS4050, 50A
Diode bridge	IXYS VUE75-12NO7, 1200V, 75A
IGBT	IRF IRG4PF50W, 900V, 51A
Output diode	IXYS DSEP 60-12AR, 1200V, 60A, 40ns
Output capacitor	680μF, 2x400Vdc
Controller	TMS320F2808 DSP board

running at 100MHz, implements the control scheme which is shown as a block diagram in Fig. 7 and is mounted on top of the power PCB.

A. Closed Loop Control

The closed loop control strategy was tested to determine its ability to directly control the input current vector. In Fig. 10 the simulated input currents for symmetric mains voltages of 115V_{RMS}/400Hz, a load of 27Ω, an output voltage of 520V and a reference current of 41A, i.e. approximately 10kW output power are depicted for a simulation model which has been implemented in Simplorer^{TM}. The resulting THD of the input current is approximately 2.8% for the simulation, which increases slightly in case the switching frequency is reduced. In Fig. 11 measured waveforms for an input current of approximately 41A for symmetrical mains voltages are shown, which demonstrate the ability of the closed loop control scheme to track a sinusoidal reference current. Due to power limitations the measurements have been performed at lower input/output voltages, but nevertheless the results demonstrate the performance of the system.

To demonstrate the ability of the control strategy to directly control the amplitude of the input current, in Fig. 12 a step change of the reference current from 26A to 46A is shown. There, also the d- and the q-component

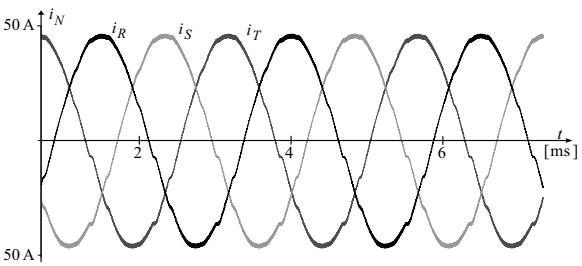

Fig. 10: Simulated input currents for symmetrical mains voltages and a switching frequency of 100kHz. The THD of the input current is ≈ 2.8%.

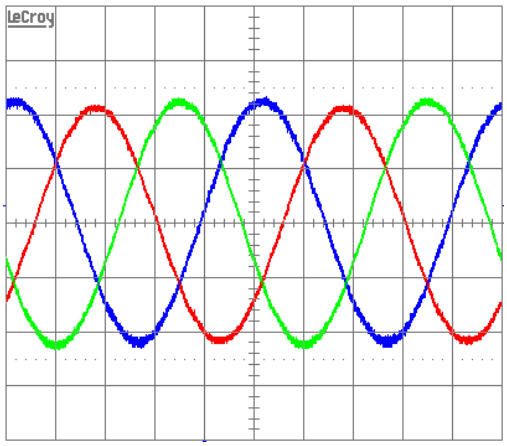

Fig. 11: Measured input currents for symmetrical mains voltages and a switching frequency of 60kHz. (Scale: 20A/div, 0.5ms/div)

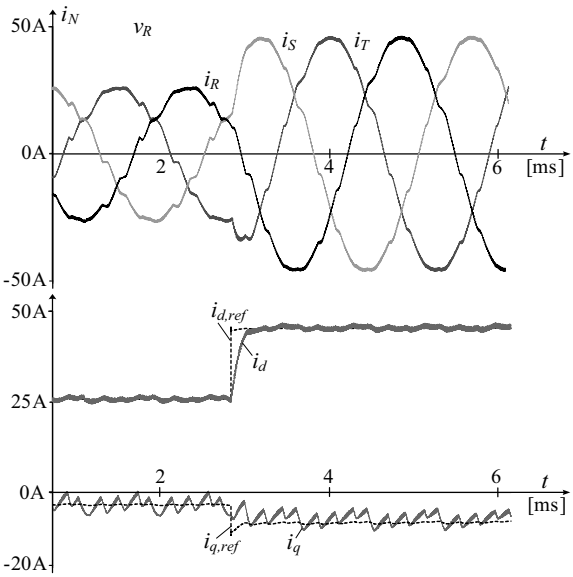

Fig. 12: Simulated input currents and d- and q-component of the mains current for a step of the reference current from 26A to 41A .

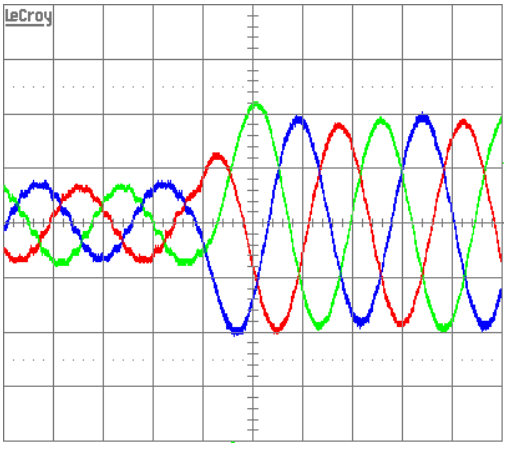

Fig. 13: Measured input currents for a step of the reference current from 15A to 40A. (Scale: 20A/div, 1ms/div)

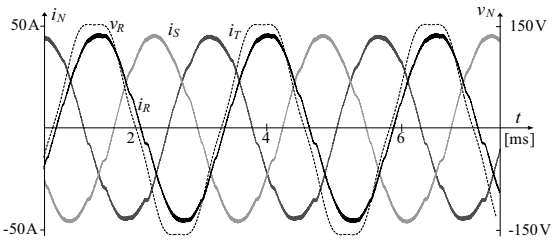

Fig. 14: Simulated input currents for mains voltages with 5% fifth harmonic and a switching frequency of 100kHz. The THD of the input current is $\approx 3.1\%$.

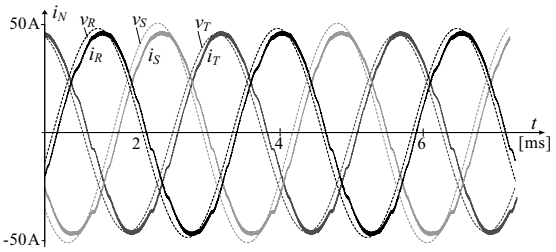

Fig. 15: Simulated input currents for unbalanced mains voltages with $152V_p$ in phase T, $160V_p$ in phase R and $168V_p$ in phase S and THD of $\approx 3\%$.

of the mains current is depicted and it can be seen that the mains current rapidly follows the reference values. The same is true for the measured load step shown in Fig. 13.

B. Asymmetric Mains/Harmonic Rejection

The strength of the closed loop current control strategy lies in its ability to track a sinusoidal reference current despite fluctuations in the input voltage. To demonstrate this feature of the current control strategy a simulation was performed with the input voltage containing 5% 5th harmonic, resulting in an input current THD of 3.1%. The simulation results are shown in Fig. 14. In case the harmonic content is increases to 10% 5th harmonic, the THD increases up to 4.7%. Since no source which is able to generate a 400Hz three phase system with fifth harmonic has been available, no measurement results for this case are shown. But the simulations, which agree very well with the measurements in the other cases, demonstrate that also in this case the rectifier system draws sinusoidal mains currents.

Also for unbalanced mains voltages the closed loop controlled 12 pulse rectifier draws sinusoidal input currents as shown in Fig. 16, where an unbalance of $\pm 5\%$ of the voltage amplitudes is assumed. There, a THD of approximately 3% results. Again, the measurement results also show for unbalanced mains voltages, that the controller is able to track a sinusoidal reference current even for unbalanced mains voltages.

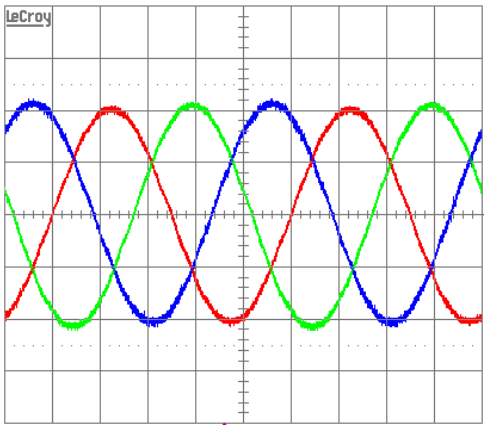

Fig. 16: Measured input currents for unbalanced mains voltages with $\pm 5\%$ asymmetry. (Scale: 20A/div, 0.5ms/div)

V. Conclusion

This paper presents a novel current control scheme for a hybrid 12-pulse rectifier employing a LIT. Starting from the basic principle of operation, the modulation functions which allow a direct control of the input current space vector are derived. The practical implementation of the control scheme is explained and experimental results are presented to demonstrate the efficacy of the control strategy. The closed loop current control scheme not only allows the converter to draw high-quality sinusoidal mains currents but also provides controllability of the current magnitude. In a next step a direct power control is implemented for the hybrid rectifier and the integration of the boost inductance in the LIT is investigated.

References

[1] C. Niermann, "New rectifier circuits with low mains pollution and additional low cost inverter for energy recovery," in *European Conference on Power Electronics and Applications, EPE'89*, vol. 3, Oct. 1989, pp. 1131–1136.

[2] K. Oguchi, G. Maeda, N. Hoshi, and T. Kubata, "Coupling rectifier systems with harmonic cancelling reactors," *Industry Applications Magazine, IEEE*, vol. 7, no. 4, pp. 53–63, July-Aug. 2001.

[3] G. Gong, M. L. Heldwein, U. Drofenik, J. Miniboeck, K. Mino, and J. W. Kolar, "Comparative evaluation of three-phase high power factor ac-dc converter concepts for application in future more aircraft," *IEEE TRANSACTIONS ON INDUSTRIAL ELECTRONICS*, vol. 52, no. 3, pp. 727–737, June 2005.

[4] K. Mino, G. Gong, and J. Kolar, "Novel hybrid 12-pulse boost-type rectifier with controlled output voltage," *IEEE Transactions on Aerospace and Electronic Systems*, vol. 41, no. 3, pp. 1008–1018, July 2005.

[5] C. N., *Netzfreundliche Gleichrichterschaltungen mit netzseitiger Saugdrossel zur Speisung von Gleichspannungszwischenkreisen*. VDI Forschrittsberichte, 1990, vol. 21, no. 68.